*International Journal of Scientific Research and Engineering Development-– Volume 9 Issue 4, July – August 2026*
*Available at www.ijsred.com*

RESEARCH ARTICLE OPEN ACCESS

# Comparative Performance Analysis of High-Temperature Hybrid Composite Coatings for Gas Turbine Blades

Dr. Shailendra Kumar Bohidar[*1], Shubham[*2]
[*1]DSc Research Scholar, Department of Research, Sikkim Sardar Patel University, Namchi, Sikkim, India, 737126
[*2]M.Tech. Research Scholar, Department of Mechanical Engineering, MATS University, Raipur, Chhattisgarh, India, 493441

----------------------------------------------------************************----------------------------------------

## Abstract:

The continuous drive to raise turbine entry temperature (TET) in gas turbine engines, in pursuit of higher thermodynamic efficiency, has pushed nickel-based superalloys beyond their inherent thermal capability. High-Temperature Hybrid Composite Coatings, and in particular advanced Thermal Barrier Coatings (TBCs), are therefore indispensable for protecting turbine blades against extreme heat, oxidation, hot corrosion and thermal shock. Conventional Yttria-Stabilized Zirconia (YSZ) coatings suffer from high-temperature sintering, Calcium-Magnesium-Alumino-Silicate (CMAS) infiltration, and spallation driven by Thermally Grown Oxide (TGO) growth stresses. This paper presents a comparative performance analysis of hybrid composite coating systems, combining a critical literature review with a finite-element-informed thermo-mechanical simulation. Four architectures — conventional YSZ/MCrAlY, a La2Ce2O7 hybrid, a Functionally Graded Coating (FGC), and a High-Entropy Oxide (HEO) hybrid — are modelled under identical thermal boundary conditions representative of a turbine blade aerofoil. Results show that hybrid and graded architectures reduce substrate temperature and, to a lesser extent, interfacial stress relative to the conventional baseline, but that TGO growth stress dominates end-of-life interfacial stress for all architectures, indicating that TGO growth control is at least as important as top-coat chemistry selection for extending coating life.

*Keywords* — **Thermal Barrier Coating; Hybrid Composite Coating; Gas Turbine Blade; Functionally Graded Coating; CMAS; Finite Element Analysis.**

----------------------------------------------------************************----------------------------------------

## I. INTRODUCTION

Gas turbine engines operate on the Brayton thermodynamic cycle, in which thermal efficiency and specific power output increase monotonically with turbine entry temperature (TET). Over the last seven decades, TET in aero and industrial gas turbines has risen from around 900°C to in excess of 1600–1700°C, made possible not merely by improvements in the base metallurgy of nickel-based superalloys — whose incipient melting points remain near 1300–1350°C — but by internal blade cooling combined with external Thermal Barrier Coatings (TBCs). A conventional TBC system consists of a superalloy substrate, a metallic MCrAlY bond coat, a Thermally Grown Oxide (TGO) scale that forms in service, and a ceramic top coat, most commonly 7–8 wt% Yttria-Stabilized Zirconia (YSZ) [1], as illustrated schematically in Fig. 1.

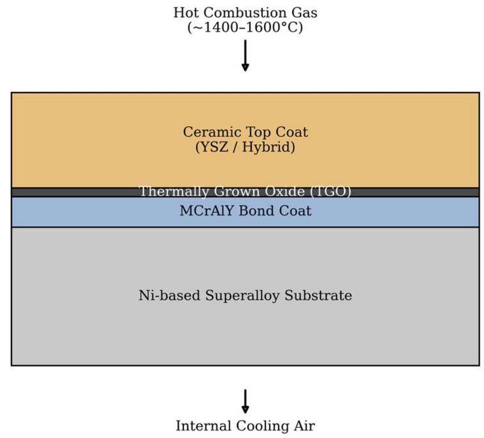


Fig. 1. Schematic cross-section of a hybrid thermal barrier coating system.

Conventional YSZ-based TBCs begin to sinter above approximately 1200°C, are thermochemically vulnerable to Calcium-Magnesium-Alumino-Silicate (CMAS) attack, and suffer spallation driven by TGO growth stress. High-Temperature Hybrid

Composite Coatings address these limitations by integrating multiple material systems — rare-earth zirconates, functionally graded architectures, nanocomposite reinforcements and high-entropy oxides — into a single protective architecture [2]. While each of these chemistries has been individually shown to improve on one or more limitations of conventional YSZ, the published literature offers little direct, quantitative, like-for-like comparison of competing hybrid architectures under a common set of thermal boundary conditions.

This paper addresses that gap by combining a critical review of the hybrid-coating literature with a finite-element-informed thermo-mechanical simulation study. Four representative coating architectures — conventional YSZ/MCrAlY, a La2Ce2O7 hybrid, a Functionally Graded Coating (FGC), and a High-Entropy Oxide (HEO) hybrid — are modelled under identical boundary conditions, and the resulting comparative trends are benchmarked against qualitative and quantitative findings reported in the literature.

Beyond aero-propulsion, such coatings extend service life and maintenance intervals of heavy-duty land-based gas turbines used in combined-cycle power plants, directly contributing to improved plant efficiency and reduced fuel consumption and emissions; they are also of growing interest for hypersonic and re-entry vehicle thermal protection, where Ultra-High-Temperature Ceramics and hybrid smart coatings are an active area of research.

## II. LITERATURE REVIEW

### *A. Chronological Review of Prior Work*

Early work established the foundational failure mechanisms of thermal barrier coatings. Sivakumar and Mordike [3] showed that laser-glazing of the ceramic surface seals the inherent porosity of plasma-sprayed coatings against hot-corrosion attack while preserving bulk insulating porosity. Goward [4] established that coating durability is governed by TGO behaviour rather than the ceramic top coat alone, and that yttrium modification of the bond coat is critical to TGO adherence. Mévrel [5] treated the coating and substrate as a single interacting chemical system, showing that interdiffusion-driven aluminium depletion from the bond coat triggers long-term failure. DeMasi-Marcin and Bhat [6] argued that strain tolerance of the ceramic layer matters more than absolute hardness, while Bernstein [7] advanced an integrated life-prediction philosophy combining oxidation, creep and fatigue.

A materials-diversification phase followed. Rusinov et al. [8] demonstrated that nanostructured layered composites with refractory reinforcement can raise heat resistance by an order of magnitude in dusty, high-salt environments. Saif, Mullick and Imam [9] showed that a three-layer NiCoCrAlY/YSZ/La2Ce2O7 hybrid provides higher thermal resistance than conventional two-layer YSZ systems. Pauzi et al. [10] highlighted CMAS infiltration as the central unsolved challenge and argued for chemically reactive coatings that trigger crystallization of molten ash. Wee et al. [11] showed that laser-induced segmentation of the top coat improves thermal-cycling life. Thakare et al. [12] proposed replacing the sharp bond-coat/top-coat interface with a continuously graded composition to eliminate the associated stress concentration. Tejero-Martin et al. [13] showed that suspension-based spray routes produce finer, more erosion- and corrosion-resistant microstructures than atmospheric plasma spraying (APS).

More recent studies have emphasised emerging chemistries and predictive methods. Bonu and Barshilia [14] introduced High-Entropy Oxides (HEOs) as configurationally stabilised, low-conductivity ceramics for extreme environments. Jude et al. [15] showed that optimised internal cooling can effectively double coating durability. Vagge and Ghogare [16] identified chromium-rich phases as effective against Type II hot corrosion. Mehta et al. [17] advocated Finite Element Analysis (FEA) and machine-learning-based prediction over trial-and-error development, showing that CMAS-type attack degrades performance primarily through the internal stress field rather than temperature change alone. Barwińska et al. [18] used Digital Image Correlation to show that interfacial de-bonding energy peaks at the aerofoil edge.

Read together, this literature shows a clear evolution from early TGO- and sealing-based failure understanding towards materials diversification and, most recently, predictive simulation-based design. Table I summarises the key contribution of each study reviewed.

TABLE I. SUMMARY OF KEY LITERATURE REVIEWED

| Ref. | Author(s) and Year | Key Contribution |
|---|---|---|
| [3] | Sivakumar & Mordike (1989) | Laser-glazing seals plasma-sprayed porosity against hot corrosion |
| [4] | Goward (1984) | TGO behaviour, not top coat, governs coating durability |
| [5] | Mévrel (1989) | Bond-coat Al depletion via interdiffusion triggers failure |
| [6] | DeMasi-Marcin & Bhat (1994) | Strain tolerance more critical than hardness |
| [7] | Bernstein (1999) | Integrated oxidation–creep–fatigue life prediction |
| [8] | Rusinov et al. (2024) | Nanostructured composites raise heat resistance ≈ 10× |
| [9] | Saif, Mullick & Imam (2019) | La2Ce2O7/YSZ hybrid outperforms two-layer YSZ |
| [10] | Pauzi et al. (2020) | Reactive coatings needed to crystallise molten CMAS |
| [11] | Wee et al. (2020) | Laser segmentation improves thermal-cycling life |
| [12] | Thakare et al. (2021) | Graded interface reduces stress concentration |
| [13] | Tejero-Martin et al. (2021) | Suspension spraying improves erosion/corrosion resistance |
| [14] | Bonu & Barshilia (2022) | High-entropy oxides: low conductivity, phase stability |
| [15] | Jude et al. (2022) | Optimised cooling can double coating durability |
| [16] | Vagge & Ghogare (2022) | Cr-rich phases resist Type II hot corrosion |
| [17] | Mehta et al. (2022) | FEA/ML prediction; CMAS acts via internal stress field |
| [18] | Barwińska et al. (2023) | DIC shows peak de-bonding energy at aerofoil edge |
| [19] | Rana (2016) | APS process parameters and performance |
| [20] | Alqallaf et al. (2020) | Acoustic emission for real-time TBC monitoring |

### *B. Research Gaps*

Despite this progress, four specific gaps remain. First, although HEOs and rare-earth zirconates show clear promise for lower conductivity and higher phase stability than YSZ [14], most published studies report only short-duration laboratory tests, and long-term (1000+ hour) industrial cycling data remain scarce. Second, coating-health assessment still relies overwhelmingly on scheduled inspection rather than continuous, in-service monitoring; techniques such as acoustic emission [20] are promising but not yet widely integrated into operational engines. Third, machine-learning erosion and life-prediction models [17] often lack physics-informed parameters capable of generalising beyond their training data, and a predictive framework applicable across multiple hybrid architectures — rather than a single composition — has not been comprehensively demonstrated. Fourth, self-healing coating concepts [12] have been demonstrated only at laboratory scale, with fabrication repeatability and qualification testing remaining the principal barriers to industrial adoption. These four gaps motivate the comparative simulation framework developed in this paper.

## III. METHODOLOGY

### *A. Coating Architectures Modelled*

Four architectures were modelled on a common Ni-superalloy substrate (1.0 mm), MCrAlY bond coat (150 µm, deposited by APS [19]) and a 300 µm ceramic top coat: (A) conventional YSZ/MCrAlY baseline; (B) a NiCoCrAlY/YSZ/La2Ce2O7 hybrid, following [9]; (C) a Functionally Graded Coating (FGC) with metal-rich, 50/50 and ceramic-rich graded sub-layers, following [12]; and (D) a YSZ/HEO hybrid, following [14]. The rare-earth and HEO outer layers of Architectures B and D were assumed deposited by EB-PVD or S-HVOF for their finer, more strain-tolerant microstructure [13].

### *B. Finite Element Discretisation*

Each architecture was discretised as a representative multilayer stack of substrate (1.0 mm), bond coat (150 µm), a TGO layer growing from 1 µm to 8 µm, and a 300 µm ceramic top coat subdivided per architecture, with local refinement at every interface (element size of order 1–2 µm) to resolve the steep interfacial temperature and stress gradients expected near the TGO and bond-coat/top-coat interfaces.

### *C. Governing Relations*

The through-thickness steady-state temperature distribution was obtained from a one-dimensional series thermal-resistance representation of the multilayer stack: $q = (T_{gas} - T_{cool}) / [1/h_{gas} + \Sigma(L_i/k_i) + 1/h_{cool}]$, where q is heat flux, $L_i$ and $k_i$ are the thickness and conductivity of layer i, and $h_{gas}$, $h_{cool}$ are the gas-side and cooling-side convective coefficients. At each interface, the CTE-mismatch thermal stress was estimated using the standard thin-film relation $\sigma_{mismatch} = [E_c/(1-\nu_c)] \times |\alpha_a - \alpha_b| \times \Delta T_{cycle}$, where $E_c$ and $\nu_c$ are the modulus and Poisson's ratio of the more brittle adjacent layer, $\alpha_a$ and $\alpha_b$ are the CTE values on either side, and $\Delta T_{cycle}$ is the swing between the local operating temperature and an assumed 25°C shut-down condition. A separate, additive TGO growth-stress term, $\sigma_{growth} = [E_{TGO}/(1-\nu_{TGO})] \times \varepsilon_{growth}$, was superimposed at the ceramic/TGO/metal location, with the growth strain $\varepsilon_{growth}$ increasing linearly with TGO thickness.

### *D. Load Cases and Comparative Metrics*

A common steady-state boundary condition (bulk gas temperature 1500°C, $h_{gas}$ = 1500 W/m²K; cooling-air temperature 400°C, $h_{cool}$ = 3000 W/m²K) was applied to all four architectures. Each architecture was evaluated at a fresh, Beginning-of-Life (BOL) TGO thickness of 1 µm and an aged, End-of-Life (EOL) thickness of 8 µm. The governing (maximum) interfacial stress across all interfaces in each stack was normalised by a common reference interfacial strength of 800 MPa to give a purely comparative spallation-risk index. Integrating real-time monitoring techniques such as acoustic emission [20] with this framework is identified as a direction for future validation.

### *E. Scope and Limitations*

This comparative assessment is subject to several simplifying assumptions: material properties are compiled as representative literature values rather than measured experimentally; the model represents a simplified multilayer cross-section rather than full three-dimensional blade geometry, and excludes rotational and platform-fixing stresses; CMAS and hot-corrosion chemistry are represented through simplified structural assumptions rather than explicit reaction-diffusion modelling; and interfaces are assumed perfectly bonded, so the resulting stresses indicate relative spallation risk rather than an absolute fracture prediction. No new physical coating deposition or laboratory testing was performed; results establish comparative trends benchmarked against the literature reviewed in Section II.

## IV. MODELING AND ANALYSIS

Fig. 2 illustrates the four layer architectures modelled. Table II lists the representative thermophysical and mechanical properties adopted for each constituent layer, compiled from the general trends reported in the literature reviewed in Section II rather than measured specifically for this study.

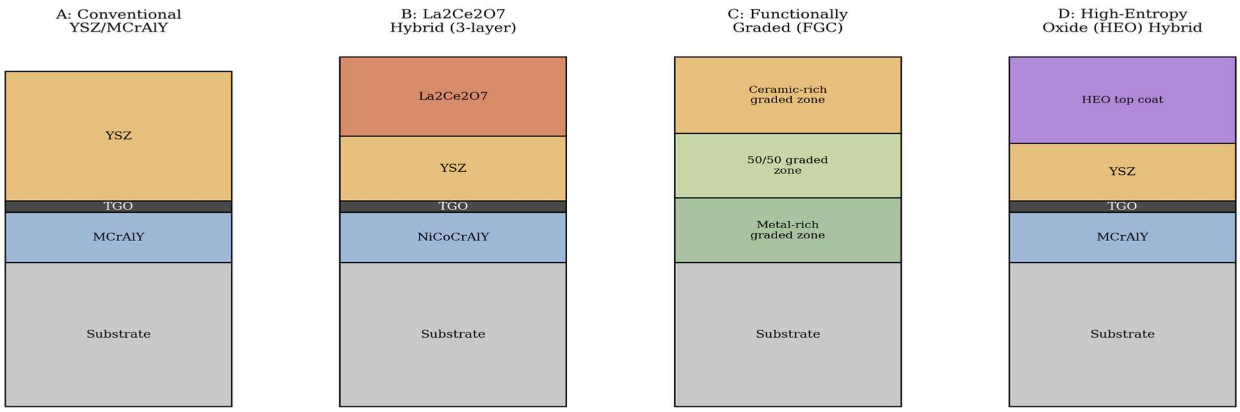


Fig. 2. Layer architectures of the four hybrid coating systems modelled.

  

TABLE II. REPRESENTATIVE MATERIAL PROPERTIES ADOPTED FOR THE FINITE ELEMENT MODEL

| Layer / Material | ρ (kg/m³) | k (W/m·K) | CTE (×10⁻⁶/K) | E (GPa) | ν |
|---|---|---|---|---|---|
| Substrate (Ni superalloy) | 8700 | 11.0 | 14.5 | 200 | 0.30 |
| MCrAlY / NiCoCrAlY bond coat | 7320 | 4.3 | 15.4 | 140 | 0.30 |
| TGO (Al2O3) | 3980 | 10.0 | 8.0 | 380 | 0.22 |
| YSZ (7–8 wt%) | 5300 | 2.0 | 10.7 | 15 | 0.15 |
| La2Ce2O7 | 6400 | 1.5 | 11.0 | 20 | 0.25 |
| HEO top coat | 6500 | 1.1 | 10.5 | 20 | 0.25 |

## V. RESULTS AND DISCUSSION

Fig. 3 shows the steady-state through-thickness temperature profile for each architecture. All four show a steep drop across the low-conductivity ceramic top coat, a gentle drop across the thin TGO and bond coat, and a more gradual drop through the substrate.

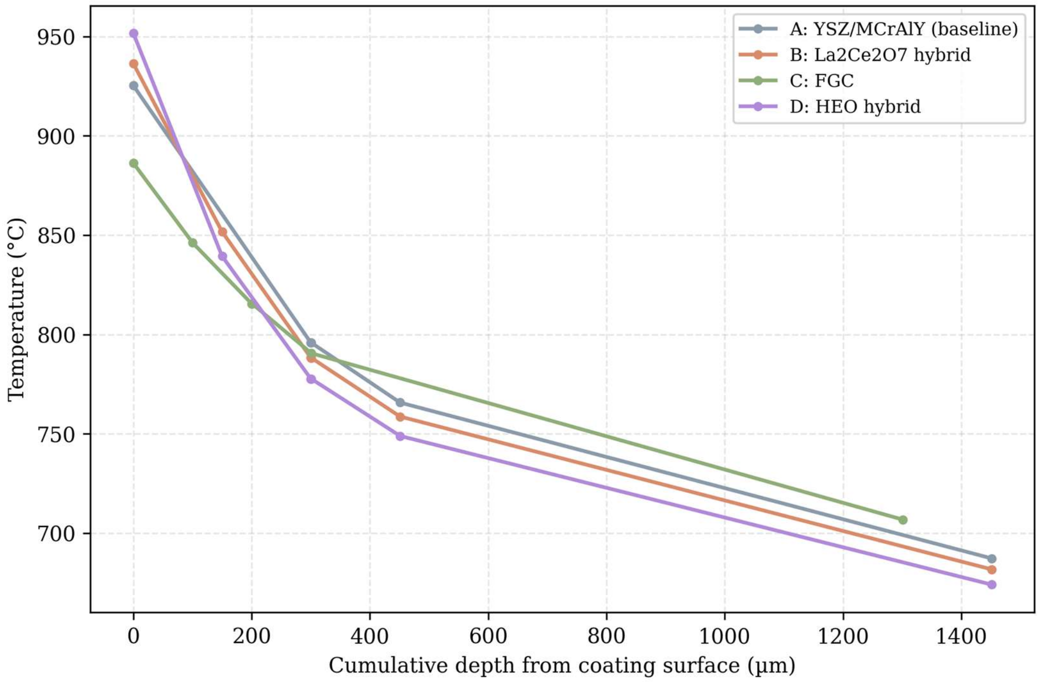


Fig. 3. Steady-state through-thickness temperature profile for the four architectures.

TABLE III. COMPARATIVE THERMAL AND INTERFACIAL-STRESS PERFORMANCE OF THE FOUR ARCHITECTURES

| Architecture | Tsubstrate (°C) | ΔTcoating (°C) | σtotal, EOL (MPa) | Risk index, EOL |
|---|---|---|---|---|
| A — YSZ/MCrAlY (baseline) | 765.8 | 159.5 | 805.5 | 1.01 |
| B — La2Ce2O7 hybrid | 758.7 | 177.6 | 799.4 | 1.00 |
| C — FGC | 790.6 | 95.7 | 804.5 | 1.01 |
| D — HEO hybrid | 749.0 | 202.6 | 798.3 | 1.00 |

  

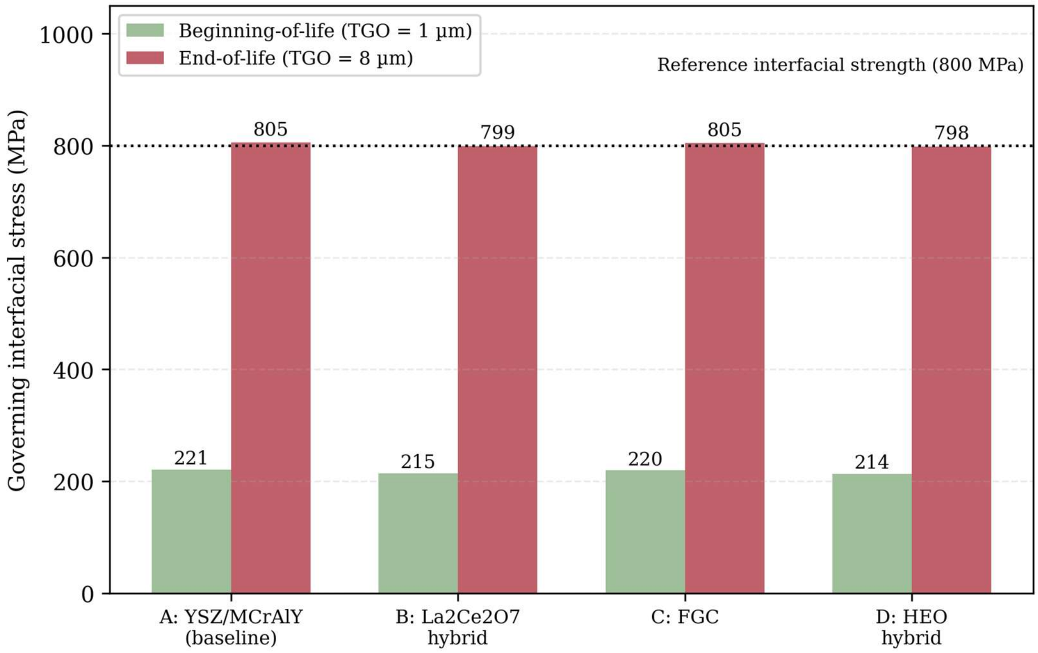


Fig. 4. Governing interfacial stress at beginning-of-life and end-of-life.

Architecture D (HEO hybrid) provides the best thermal insulation of the four systems, reducing substrate temperature by 16.8°C relative to the conventional baseline, consistent with the low thermal conductivity reported for HEO ceramics [14]. Architecture C (FGC), however, shows the weakest insulation (ΔTcoating of only 95.7°C) because its graded sub-layers retain a higher metallic — and therefore more conductive — fraction than a dedicated ceramic top coat, indicating that its principal benefit lies in mechanical stress redistribution rather than enhanced insulation, refining the interpretation of [12].

At BOL, all architectures show comparable, low interfacial stress (214–221 MPa, risk index 0.27–0.28). By EOL, the governing stress for every architecture rises to within a few percent of the reference strength (risk index 1.00–1.01), driven almost entirely by TGO growth stress, which increases from 146.2 MPa to 730.8 MPa as the TGO thickens from 1 µm to 8 µm — far larger than the 68–75 MPa spread attributable to top-coat chemistry differences between architectures. This confirms, and quantifies, the foundational arguments of Goward [4] and Mévrel [5] that TGO behaviour, rather than top-coat chemistry, ultimately governs coating life, and is consistent with the emphasis placed by Mehta et al. [17] on the internal stress field as the principal driver of degradation.

TABLE IV. OVERALL COMPARATIVE RANKING OF THE FOUR ARCHITECTURES

| Architecture | Thermal Insulation | EOL Interfacial Stress | CMAS Resistance (Literature) |
|---|---|---|---|
| A — Baseline | Reference | Reference (805.5 MPa) | Reference (susceptible) |
| B — La2Ce2O7 | Better than baseline | Marginally better | Improved (reactive sealing) |
| C — FGC | Worse than baseline | Comparable to baseline | Not primarily targeted at CMAS |
| D — HEO | Best of the four | Marginally better | Improved (entropy-stabilised) |

Table IV summarises the overall standing of the four architectures against the criteria examined. No single architecture is superior on every criterion: Architecture D offers the best thermal insulation and among the lowest EOL interfacial stress, making it attractive where long-term data availability is not a limiting factor; Architecture B offers a similar, more moderate improvement with a more established literature and manufacturing base; and Architecture C trades thermal insulation for a more distributed stress field, a benefit best realised where interfacial cracking rather than substrate overheating is the dominant concern.

## VI. CONCLUSION

A combined literature-review and finite-element-informed simulation framework was used to compare four high-temperature hybrid composite coating architectures for gas turbine blades under identical thermal boundary conditions. The High-Entropy Oxide hybrid provided the best thermal insulation and among the lowest end-of-life interfacial stress, while the Functionally Graded Coating traded thermal insulation for a more distributed stress field. Across all four architectures, TGO growth stress — rather than top-coat chemistry — was found to dominate end-of-life interfacial stress, indicating that TGO growth control is at least as important as top-coat architecture selection for extending coating life. No single architecture was superior on every criterion, so selection should be guided by the dominant failure mode expected in service. Future work should extend the model to full three-dimensional blade geometry with rotational loading, incorporate explicit CMAS reaction-diffusion chemistry, and validate the comparative trends against burner-rig thermal-cycling data.

The principal contribution of this work is a reusable, internally consistent comparative simulation framework, together with a quantitative demonstration that TGO growth — rather than top-coat chemistry — governs end-of-life interfacial stress across all four architectures studied, and a clarification that the functionally graded architecture's benefit lies primarily in stress redistribution rather than enhanced thermal insulation.

## ACKNOWLEDGMENT

The authors gratefully acknowledge the support and guidance of the Department of Mechanical Engineering, MATS University, Raipur, in carrying out this research.

## REFERENCES

[1] R. Darolia, “Thermal barrier coatings for high temperature gas turbine engines,” *International Materials Reviews*, vol. 58, no. 6, pp. 315–348, 2013.

[2] Y.-L. Yang et al., “High-temperature oxidation-resistant composite coatings for extreme environments: Material systems, design strategies, preparation technologies, performance characterizations, and research challenges,” *Journal of Composites Science*, vol. 10, no. 1, p. 51, 2026.

[3] R. Sivakumar and B. L. Mordike, “Laser surface treatment of plasma sprayed thermal barrier coatings,” *Surface and Coatings Technology*, vol. 37, no. 2, pp. 139–151, 1989.

[4] G. W. Goward, “Low-pressure plasma-sprayed coatings for high-temperature corrosion resistance,” *Journal of Metals*, vol. 36, no. 10, pp. 32–39, 1984.

[5] R. Mévrel, “State of the art in high-temperature corrosion-resistant coatings,” *Materials Science and Engineering: A*, vol. 120, pp. 13–24, 1989.

[6] J. T. DeMasi-Marcin and T. N. Bhat, “Failure mechanisms of plasma-sprayed thermal barrier coatings,” *Surface and Coatings Technology*, vol. 68–69, pp. 1–9, 1994.

[7] H. L. Bernstein, “Life prediction of thermal barrier coatings for industrial gas turbines,” *Journal of Engineering for Gas Turbines and Power*, vol. 121, no. 2, pp. 276–283, 1999.

[8] P. Rusinov, G. Kurapov, A. Rusinova, M. Semadeni, and P. Sereda, “Influence of high-temperature aggressive environments on the durability of composites reinforced with refractory particles,” *Metals*, vol. 14, no. 8, p. 939, 2024.

[9] M. Saif, P. Mullick, and A. Imam, “Nanostructured hybrid coatings for gas turbine applications: A review,” *Materials Today: Proceedings*, vol. 18, pp. 5214–5221, 2019.

[10] A. A. Pauzi, M. J. Ghazali, W. F. H. W. Zamri, and A. Rajabi, “CMAS mitigation strategies for thermal barrier coatings: A review of material and microstructural perspectives,” *Journal of*

  

*Materials Research and Technology*, vol. 9, no. 6, pp. 14603–14620, 2020.

[11] S. Wee, J. Do, K. Kim, C. Lee, C. Seok, B. G. Choi, and W. Kim, “Segmented thermal barrier coatings via laser surface melting for enhanced thermal cycling life,” *Surface and Coatings Technology*, vol. 399, p. 126154, 2020.

[12] J. G. Thakare, C. Pandey, M. M. Mahapatra, and R. S. Mulik, “Functionally graded hybrid thermal barrier coatings: A review on processing and performance,” *Ceramics International*, vol. 47, no. 11, pp. 14819–14838, 2021.

[13] D. Tejero-Martin, C. Bennett, and T. Hussain, “A review on environmental barrier coatings: History, current state of the art and future developments,” *Journal of the European Ceramic Society*, vol. 41, no. 3, pp. 1747–1768, 2021.

[14] V. Bonu and H. C. Barshilia, “High-entropy oxide coatings for extreme environments: Evolution, challenges, and future directions,” *Journal of Alloys and Compounds*, vol. 918, p. 165681, 2022.

[15] S. A. A. Jude, J. T. W. Jappes, and M. Adamkhan, “Experimental investigation on hot corrosion resistance of HVOF sprayed hybrid WC-Co coatings,” *Materials Today: Proceedings*, vol. 51, pp. 1422–1428, 2022.

[16] S. T. Vagge and S. Ghogare, “Hot corrosion studies of Al2O3-reinforced hybrid Ni-based coatings in molten salt environments,” *Journal of Thermal Spray Technology*, vol. 31, pp. 842–855, 2022.

[17] A. Mehta, H. Vasudev, S. Singh, C. Prakash, K. K. Saxena, E. Linul, D. Buddhi, and J. Xu, “Machine learning and finite element analysis in the prediction of erosion behavior of hybrid coatings,” *Coatings*, vol. 12, no. 3, p. 350, 2022.

[18] I. Barwińska, M. Kopeć, D. Kukla, C. Senderowski, and Z. L. Kowalewski, “Evaluation of the mechanical properties and fatigue life of protective coatings for single crystal superalloys,” *Materials Science and Engineering: A*, vol. 862, p. 144456, 2023.

[19] H. M. Rana, “Air plasma spraying (APS) techniques for thermal barrier coatings: Parameters and performance,” *International Journal of Mechanical Engineering*, vol. 5, no. 2, pp. 45–58, 2016.

[20] J. Alqallaf, N. Ali, J. A. Teixeira, and A. Addali, “Acoustic emission monitoring of thermal barrier coating failure mechanisms: A review,” *Sensors*, vol. 20, no. 1, p. 123, 2020.